EARTHQUAKE OBSERVATION OF A LOW-RISE BUILDING

Yuzuru Yasui, Takeshi Fujimori and Kunio Wakamatsu

Technical Research Institute, Obayashi Corporation, Tokyo, Japan
E-mail: y.yasui@tri.obayashi.co.jp

ABSTRACT

Observation data from the Hyogo-ken Nanbu earthquake have indicated that the building foundation responses were generally small compared with ground surface responses. Moreover, building damage was small even though the earthquake greatly exceeded the design level. This is thought to be concerned with the interaction effect, and there is a view that especially low-rise building should have received the benefit of reducing the damage. However, that view has not yet been directly confirmed by large earthquake records. Therefore, earthquake observations are required that demonstrate the behavior of low-rise buildings in large earthquakes. This report first introduces earthquake observation results of a certain low-rise building. Then it examines the interaction effects for a future large earthquake like the Great Kanto earthquake.

KEYWORDS

Soil-structure interaction effect, low-rise building, earthquake observation, the Kanto earthquake and response analysis

1. INTRODUCTION

It has been shown that there was also an interaction effect in a large earthquake like the Hyogo-ken Nanbu earthquake [Yasui, 1996; Yasui et al., 1998]. However, some analytical studies have also been performed in order to determine if there is an interaction effect during large earthquakes. Results of these studies have indicated that the effect varies with the type of earthquake motion [Hayashi et al., 2000 ; Hayashi et al.,2001]. In order to clarify this question, it is necessary to carry out earthquake observations of low-rise buildings to determine their behavior during large earthquakes [Fukuwa and Tobita, 2000]. This report first describes a building where earthquake observations were carried out, and the surrounding ground. Next, records of small earthquakes currently measured until now are analyzed, and the interaction effect is examined. Furthermore, calculations are performed to determine what motion the building would have shown during the Great Kanto Earthquake, which it is assumed might recur in the future.

2. OUTLINE OF BUILDING AND GROUND

The target site is in Kiyose-shi, Tokyo, as shown on the map in Figure 1. The subject building has one story below ground level, three stories above ground, and one story penthouse, and is made of reinforced concrete. It is a management building of a research institute. It is about 16m high, its standard story height is 3.2m, and its plan size is 36mx21.6m. Figure 2 shows a sectional view in the short direction and a plan view. The south of the building comprises a dry area about 3m deep, and the first floor wall on the north side is covered with landfill to a height of about 2m, as shown in the sectional view. The seismograph positions are also shown in the sectional view. Two are inside the building and three are in the ground. The measurement direction consists of two horizontal components and one vertical component at each observation point. The horizontal components are aligned with the longitudinal and short span directions of the building. The ground soil profile and the fundamental parameter values are shown in Table 1. The ground has the Kanto loam layer to a thickness of about 5m from the surface. The S-wave velocities (Vs) for the observed earthquake to a depth of 15m, shown in Table 1, were defined on the basis of logging test results. The lower ground comprises a multi-layer structure of gravel layers, fine sand layers, and clay layers at least to a depth of 180m [Nakagawa et al., 1972]. The profile of layers below GL-15m and their S-wave velocities are defined on the basis of seismic reflection profiling test results in Fuchu-shi, Tokyo [Asano et al, 1994], and attenuation values (h) are defined as 10/Vs.

3. OBSERVATION RECORDS AND SIMULATION ANALYSES

Since earthquake observations started in April, 1998, the one that produced the biggest acceleration occurred on August 29, 1998. The epicenter of this earthquake was in Tokyo Bay, its magnitude was 5.1, its depth of focus was 67km, and its epicentral distance was 38.7km. Its epicenter is shown in Figure 1. Some of its recorded waveforms are shown in Figure 3. These waveforms were in the span direction of the building, henceforth expressed as the NS direction. The maximum acceleration of the ground surface (GL-0.8m) was 41.1 gals, and the maximum acceleration at the building roof was 36.5 gals. The velocity spectra (h= 0.03) of these records are shown in Figure 4. The peak at a little less than 0.2 seconds was the natural frequency of the soil surface layer (refer to Fig. 5), and the peak at a little less than 1 second is from the component contained in the earthquake input wave itself. The small peak at the foot of the big peak at a little less than 0.2 seconds near one a little less than 0.3 seconds of RF and BF is the peak produced by the soil-structure interaction. The transfer function (GL-0.8m/GL-15m) of the ground is shown in Figure 5. That transfer function has a peak of 5.5Hz. The transfer function (BF/GL-0.8m) to the ground surface of the building basement is shown in Figure 6. That transfer function corresponds to the input loss effect.

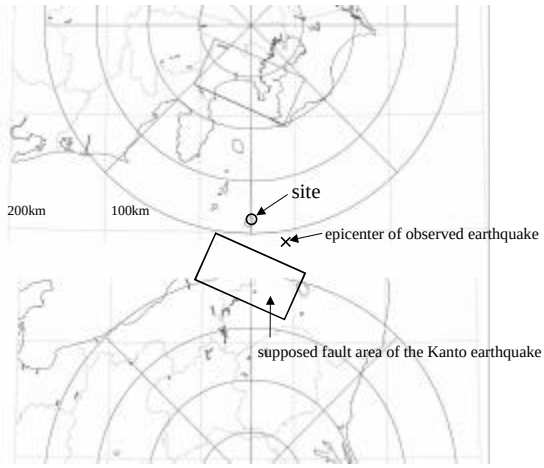

Figure 1: Epicenter of observed earthquake and assumed fault area of the Kanto earthquake

Table 1: Soil parameters

depth(m)	geologic time	soil classification	density (ton/m^3)	for observed earthquake		for the Kanto earthquake	
				V_s (m/sec)	h	V_s' (m/sec)	h'
GL 0-0.8	Pleistcene	fill	1.45	80	0.02	63	0.055
0.8-2.2		loam	1.45	90	0.02	69	0.094
2.2-3.6			1.45	145	0.02	112	0.075
3.6-5.0			1.45	190	0.02	147	0.063
5.0-5.23		clay	1.55	240	0.02	214	0.043
5.23- 6.0			1.55	240	0.02	213	0.043
6.0-11.5		gravel	2.00	360	0.0278	360	0.0278
11.5-15		fine sand	2.00	510	0.0196	510	0.0196
15-90		sand, clay & gravel	2.00	510	0.0196	510	0.0196
90-200			2.00	550	0.0182	550	0.0182
200-310			2.00	700	0.0143	700	0.0143
310-650			2.00	840	0.0119	840	0.0119
650-1050			2.10	970	0.0103	970	0.0103
1050-1450	Miocene		2.20	1150	0.0087	1150	0.0087
1450-2020			2.30	1400	0.0071	1400	0.0071
2020-	Pre-Tertiary Basement		2.50	2950	0.0034	2950	0.0034

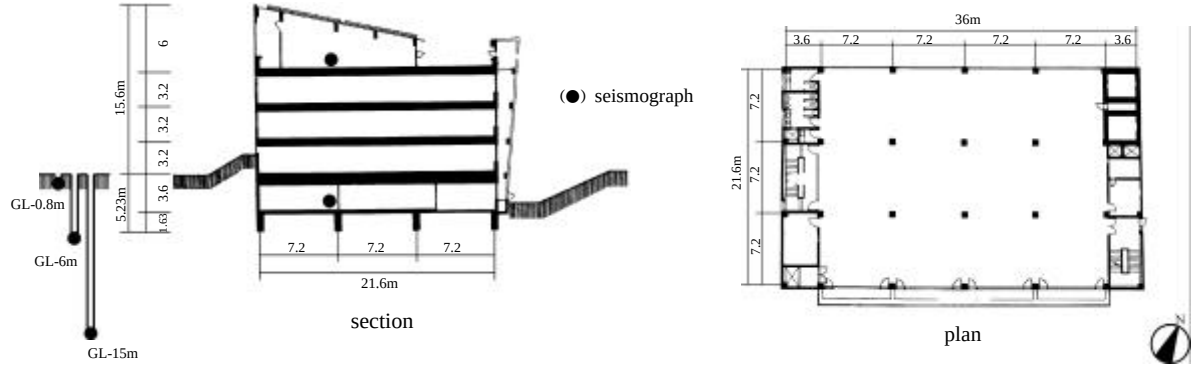

Figure 2: Plan and sectional view of building

A simulation analysis is performed for the earthquake observation result on the NS direction. The analysis model is a sway-rocking model, as shown in Figure 7. The structure model is a lumped 4-mass system, and is the equivalent shear-deformation-type model. The model foundation is assumed to be a rigid body. The parameters of the analysis model are shown in Table 2. Impedance and foundation input motion functions relevant to the interaction are estimated by the Thin Layer Element Method [Takano et al., 1988]. As the response calculation method, a technique is used that considers the frequency dependence of those functions [Hayashi and Katsukura, 1990]. The foundation input motion is used as the input seismic wave to the sway-rocking model (SR model), and the foundation input motion is evaluated by considering the kinematic interaction using the observation wave at the ground surface. The response calculation for the model to which the base of the structure is fixed is also performed for reference. For the fixed model, two cases are assumed: where the observation wave at the ground surface (GL-0.8m) is input (F1 model), and where the observation wave of the ground at the basement bottom (GL-6m) is input (F2 model).

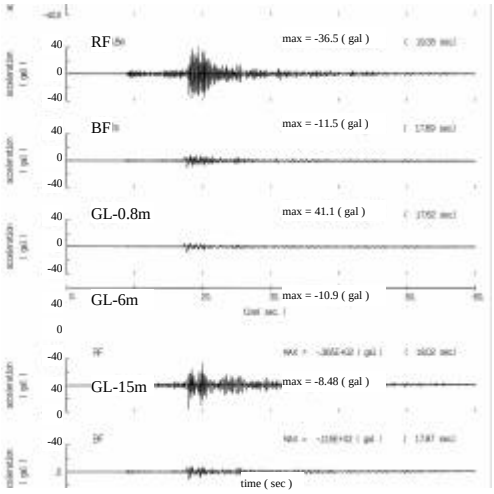

Figure 3: Observed records

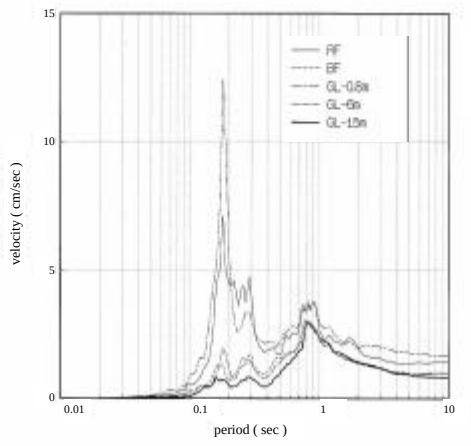

Figure 4: Velocity response spectra of observed records (h=0.03)

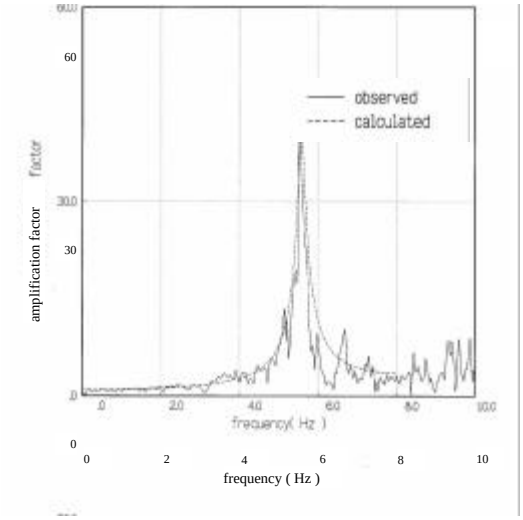

Figure 5: Amplification factor of the ground (GL-0.8m / Gl-15m)

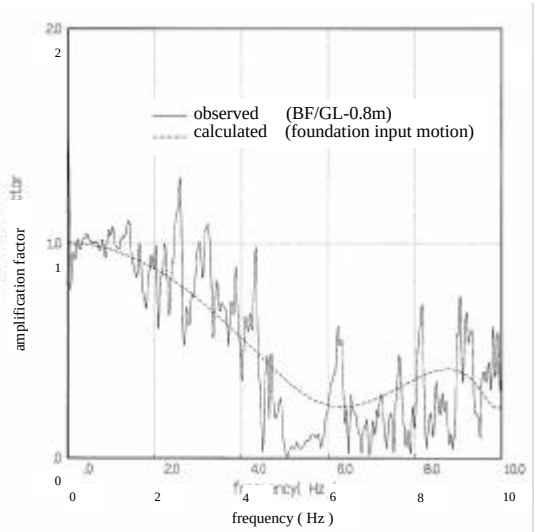

Figure 6: Spectrum ratio of BF to GL-0.8m

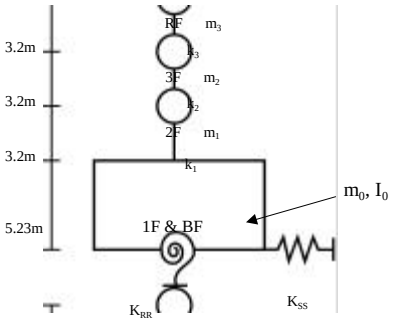

Figure 7: Sway-Rocking model

Table 2: Parameters of lumped mass model

floor	mass No.	weight (ton)	rotational inertia (ton・m^2)	elastic rigidity (ton/m)
RF	m_3	526.4	—	
				1.87×10^5
3F	m_2	526.4	—	
				1.87×10^5
2F	m_1	526.4	—	
				1.87×10^5
1F & BF	m_0	961.5	4.29×10^5	

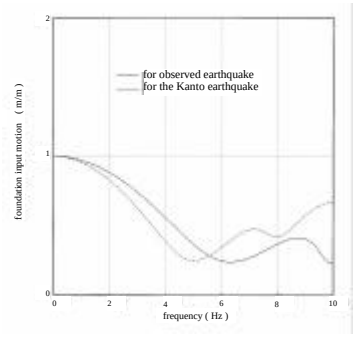

Figure 9: Input motions of the foundation

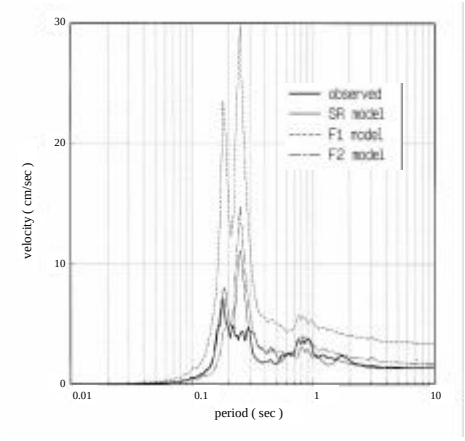

Figure 11: Comparison of response spectra (RF)

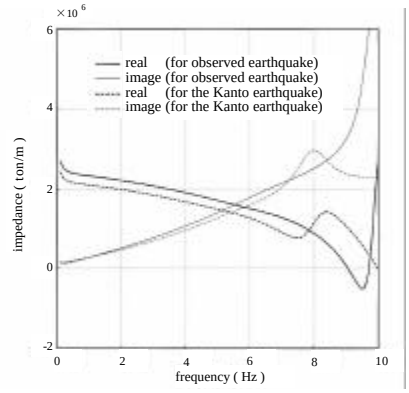

(a) Swaying (K_{SS})

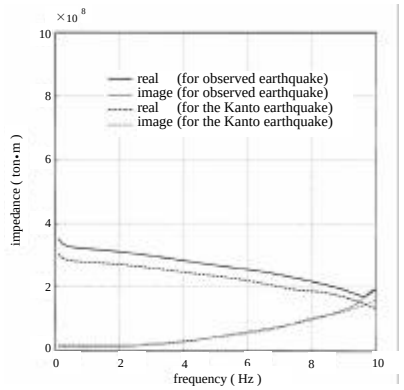

(b) Rocking (K_{RR})

Figure 8: Impedance functions of the foundation

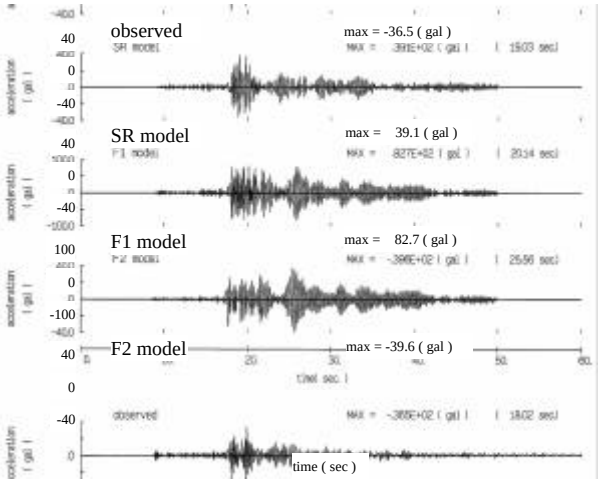

Figure 10: Comparison of waveforms (RF)

First, the simulation analysis result for the ground is shown. The calculation was made using the program SHAKE. The results are shown in Figure 5, along with the observation result. The sway-rocking impedance functions are shown in Figure 8. Figure 9 shows the transfer function to the free ground surface motion of the excavated ground surface motion, and expresses the kinematic interaction effect. Correspondence with observation value (B1F/GL-0.8m) is shown in Figure 6. The response waveforms at the roof story of the building are shown in Figure 10. Figure 11 shows the velocity response spectra (h= 0.03) of these response waveforms. The results obtained from the SR model are in good agreement with the observation values. However, the result of the SR model overestimates the interaction system peak near 0.25 seconds. This is considered to be because the analysis model does not consider the influence of the dry area and the landfill. Figures 10 and 11 show that accurate evaluation is also obtained with the F2 model.

4. RESPONSE TO ASSUMED GREAT EARTHQUAKE

The Kanto earthquake is assumed as the subject great earthquake. The Matsu'ura model [Matsu'ura et al., 1980] is used as the fault model. The assumed fault region is shown in Figure 1. It is assumed that destruction progresses in a bi-lateral direction from the center of the fault region. The seismic wave in the earthquake basement directly under the site is calculated using the semi-empirical method [Kobayashi and Midorikawa, 1982]. The S-wave velocity structure of the ground directly under the observation site containing the earthquake basement is shown in Table 1. Here, the earthquake basement is the surface of the Pre-Tertiary Basement (Vs=2,950m/s layer) of GL-2020m (refer to Table 1). The surface layer motions required for the building response calculation are calculated using SHAKE, and the convergence calculation is performed using the soil constants for the small earthquakes of Table 1 (for the observed earthquakes) as the initial values. Layers deeper than GL-6m are assumed to be elastic. In addition, the relation between shear rigidity (G) and attenuation of the ground soil (h), and shear strain (γ) are defined by the R-O model. Convergence values are shown in Table 1 for the Kanto earthquake. The transfer functions of the surface ground to the earthquake basement are shown in Figure 12. The transfer function for the initial and converged values is shown. The figure indicates that the natural period of the soil surface is somewhat elongated.

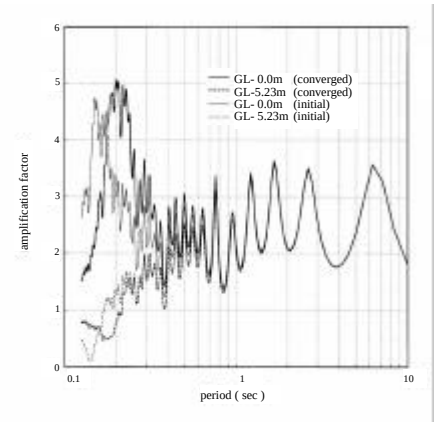

Figure 12: Amplification factor of the ground to earthquake basement

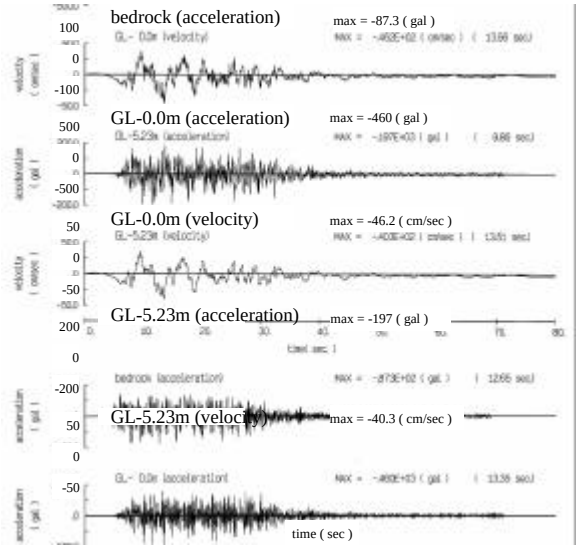

Figure 13: Waveforms of the Kanto earthquake

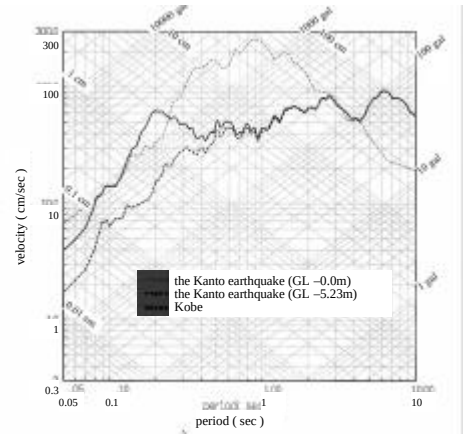

Figure 14: Response spectra of the Kanto earthquake

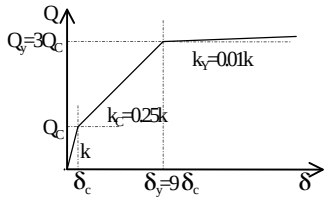

Figure 15: Force-displacement relationship

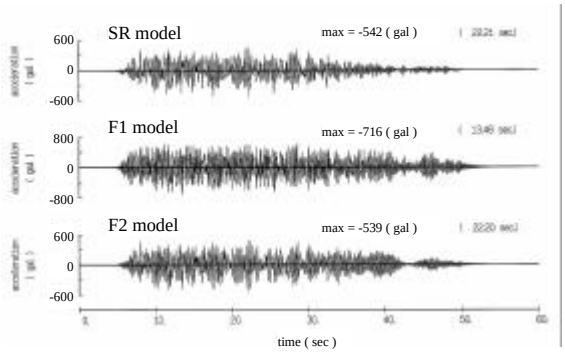

Figure 16: Response waveforms to the Kanto earthquake (RF)

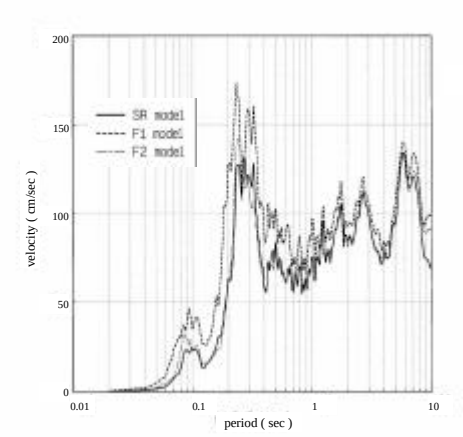

Figure 17: Velocity response spectra of computed motions for the Kanto earthquake (RF)

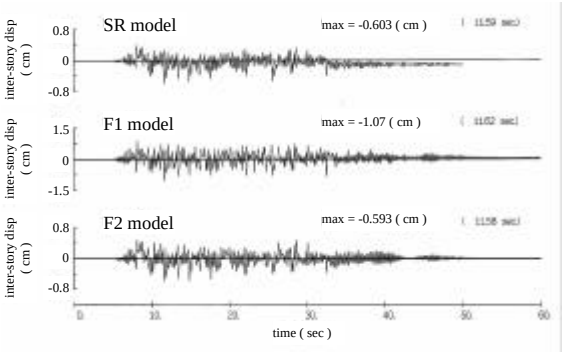

Figure 18: Response waveforms of inter-story displacement of the 1st story

Table 3: Maximum response values

floor	mass No.	model	maximum acceleration (gal)	maximum interstory displacement (cm)	ductility factor
RF	m_3	SR	542	—	—
		F1	716	—	—
		F2	543	—	—
3F	m_2	SR	387	0.154	0.0963
		F1	724	0.228	0.143
		F2	433	0.156	0.098
2F	m_1	SR	425	0.276	0.173
		F1	629	0.726	0.453
		F2	492	0.289	0.181
1F & BF	m_0	SR	262	0.603	0.377
		F1	460	1.07	0.668
		F2	171	0.595	0.372

The incidence wave to the earthquake basement, the seismic wave of GL-5.23m (depth of the basement bottom), and the ground surface are shown in Figure13. The velocity spectra (h= 0.05) are shown in Figure 14. The spectrum of the seismic wave (the NS direction) in the Kobe Marine Meteorological Observatory for the Hyogo-ken Nanbu earthquake is also shown in the figure for reference. The maximum ground surface velocity of the seismic wave used in this analysis is 46cm/sec, which is about one half that in Kobe (91cm/sec). It is noted that the velocity spectrum of the seismic wave of Kobe shows geater power.

The sway-rocking impedance functions and the input motion of the foundation for the Kanto earthquake are shown in Figure 8 and Figure 9, respectively. The restoring force characteristics of the superstructure (Q-δ relation) are assumed to be of the Normal Tri-linear type. The Q-δ relationship is shown in Figure 15. As shown, the decreasing rates of the 2nd slope and the 3rd slope to the elastic rigidity are set as one fourth and 1/100, respectively. Furthermore, yielding load (Qy) is assumed as the load where the interlayer displacement angle is 1/200, and the cracking load (Qc) is assumed to be one ninth of the yielding load. Internal damping is 2%, and is proportional to the instantaneous rigidity of the superstructure.

Calculations were performed by SR model, F1 model, and F2 model. The acceleration response waveforms of the building's RF story are shown in Figure 16. Their velocity response spectra are shown in Figure 17. Compared with the case of the small earthquake, there was little difference between the F1 model and the SR model. The F1 model's superstructure becomes much less linear compared to the SR model's superstructure. This is considered to be because the hysteresis damping increases and the response is suppressed. Table 3 shows the maximum response values. The maximum ductility factor of 0.668 is produced on the first floor of the F1 model, and the corresponding value for the SR model is 0.377.The maximum base shear force is 749 ton for the F1 model, and 531 ton for the SR model. These values show that the interaction effect cannot be disregarded. Futhermore, the maximum ductility factors are smaller than 1, and no story would reach yielding load in the Great Kanto Earthquake. The responses for the SR model and the F2 model are found to be almost equal. This shows that a result equivalent to that for the SR model may be obtained by inputting the ground earthquake motion at the bottom of basement into the base-fixed structure model [Yasui et al.,1998]. Since the response waveforms of the interlayer displacement shown in Figure 18 show different aspects from the SR model and the F2 model, further examination is required.

5. CONCLUDING REMARKS

Earthquake observation results were shown for a low-rise building. A remarkable interaction effect was recognized in the observed earthquake. Next, the interaction effect for the Kanto earthquake was examined, and it was shown that it couldn't be disregarded. Moreover, the possibility was also shown of a simple evaluation method where a ground earthquake motion at the basement bottom position is input into the base-fixed model.

As these research results showed, earthquake damage to low-rise buildings must be related and examined together with the interaction effect. Thus, to examine building damage directly from the earthquake observation record, the measuring point arrangement introduced in this paper is not enough. Ideally, it is necessary to install a horizontal sensor in each story, and to also install a vertical sensor to separate the rocking component of the foundation. Moreover, as in the example described here, when the foundation support is not regular, it is necessary to arrange sensors so that the foundation motion can be evaluated. In addition, it cannot be overemphasized that it is necessary to carry out earthquake observations of the site ground.

6. ACKNOWLEDGEMENT

The authors wish to express their gratitude to Mr. H. Hasegawa of Trans-Cosmos Inc. for his helpful corporation in

drawing the figures.

7. REFERENCES

Asano, S., K. Wakamatsu, S. Okuda, T. Kuwabara, et al. (1994). " Seismic reflection profiling in the Tokyo Metropolitan Area, " *Proceedings of The 9th Japan Earthquake Engineering Symposium*, pp.673-678, (in Japanese).

Fukuwa,N. and J. Tobita (2000). " Seismic observation of soil structure interaction system, " *The 2nd Symposium on Utilization of Strong Ground Motion data*, AIJ, pp.57-68, (in Japanese).

Hayashi, Y. and Y. Katsukura (1990). " Effective time-domain soil-structure interaction analysis based on FFT algorithm with causality condition, " *J. of Earthq. Engrg and Structural Dynamics*, vo.19, pp.693-708.

Hayashi, Y., T. Fujimori, Y. Yasui and M. Iguchi (1999). " Effects of soil-structure interaction in heavily damaged zone in the 1995 Hyogo-ken Nanbu Earthquake, " *J. of Struct. And Constr. Engrg*, AIJ, No.520, pp.45-51, (in Japanese).

Hayashi, Y., Y. Yasui and I. Takahashi (2001). " Soil-Structure Interaction and response of superstructure, " *The 6th Symposium on Soil-Structure Interaction*, AIJ, (to be published, in Japanese)

Kobayashi, H. and S. Midorikawa (1982). " A semi-empirical method for estimating response spectra of near-field ground motions with regard to fault rupture, " *Proceedings of the 7th European Conference on Earthquake Engineering*, pp.161-168.

Matsu'ura, M., T. Iwasaki, Y. Suzuki and R. Sato (1980). " Statical and dynamical study of faulting mechanism of the 1923 Kanto earthquake, " *J. of Phys. Earth*, vol.28, pp.119-143.

Nakagawa, K., T. Tsunoda and K. Seo (1972). " Problems on soil layer construction to the earthquake ground motion characteristic - Seismic refraction survey and seismic observations in Kiyose-city-, " *Report of the Technical Research Institute*, Ohbayashi-gumi, Ltd., No.6, pp.77-81, (in Japanese).

Takano, S., Y. Yasui, T. Takeda and A.Miyamoto (1988). " The new method to calculate the response of layered half-space subjected to obliquely incident body wave, " *Proceedings of the 9th World Conference on Earthquake Engineering*, pp.423-428.

Yasui, Y. (1996). " Effects of soil-structure interaction, " *First Symposium on the Hyogo-ken Nanbu Earthquake*, The Special Research Committee of the Hyogo-ken Nanbu Earthquake, AIJ, pp19-22, (in Japanese).

Yasui, Y., M. Iguchi, H. Akagi, Y. Hayashi and M. Nakamura (1998). " Effective input motion to structures in heavily damaged zone in the 1995 Hyogo-ken Nanbu Earthquake, " *J. of Struct. And Constr. Engrg*, AIJ, No.512, pp.111-118, (in Japanese).